# Supporting Information

# A zinc coordination supramolecular network synergized manganese dioxide achieves high-rate lithium-sulfur batteries

Zhao Chen, Yuanming Tan, Zengren Tao, Kaiji Lin, Shimei Lai, Shaowei Ho, Chunshan Zhou, and Yangyi Yang*

## GITT measurement

The $D_{Li+}$ was calculated based on the equation: $D_{Li+} = 4/\pi\tau\ (nV/A)^2\ (\Delta E_s/\Delta E_t)^2$, where $\tau$, n, V, and A are relaxation time, molar weight, molar volume, and geometric area of the electrode, respectively. $\Delta E_s$ and $\Delta E_t$ are potential changes that occurred in steady-state and current pulse, respectively. A current pulse of 0.2 C was applied for 0.5h min while the following relaxation time was 1h in LSBs.

## Polysulfide adsorption experiment

Zn-CSN@$MnO_2$, Zn-CSN, and $MnO_2$ powders were respectively added to the sealed glass bottle, and 0.01 M $Li_2S_6$ electrolyte was added. The ability of Zn-CSN@$MnO_2$, Zn-CSN, and $MnO_2$ to adsorb polysulfides was examined with a UV-VIS spectrometer (RIGOL Ultra-3660). $Li_2S_6$ solution was prepared by adding sulfur and $Li_2S$ into DME solution with a molar ratio of 5：1 and stirring at 50 ºC for 12 hours.

## Symmetrical battery test

Zn-CSN@$MnO_2$ electrode was prepared by mixing Zn-CSN@$MnO_2$, Ketjen black, PVDF at the weight ratio: 7:2:1 in N-methylpyrrolidone (NMP) to form homogeneous flurry and evenly cast on carbon paper with doctor blades, which was dried at 60 °C for 12 h. The two identical electrodes were assembled into a coin cell with a PP Celgard membrane as the separator. 30 μL as-prepared $Li_2S_6$ solution (0.1M) was used as the electrolyte. CV tests of symmetric cells were performed at a scan rate of 1 mV/s with the voltage ranging from −1 to 1 V.

## $Li_2S$ nucleation and dissolution test

First, 0.2 M $Li_2S_8$ electrolyte was prepared by adding sulfur and $Li_2S$ into DME solution with a molar ratio of 5：1 and stirring at 50 ºC for 12 hours. Ethanol solution of Zn-CSN@$MnO_2$, Zn-CSN, and $MnO_2$ (1 mg/mL) was dropped onto carbon paper to obtain the cathode. For the $Li_2S$ nucleation, coin-type cells (CR2025) were assembled with the commercial Celgard2500 as the separator, and the lithium foil as anode. 25 μL $Li_2S_8$ electrolyte was added to the cathode side, and 25 μL1M LiTFSI electrolyte was added

to the lithium anode side. The batteries were first discharged to 2.13 V at 0.134 mA followed by maintaining at 2.12 V until the current was below $1\times10^{-5}$ A. For the $Li_2S$ dissolution tests, the cells were assembled with identical electrolytes, separators and electrodes. Firstly, the cells were galvanostatically discharged to 1.7 V at 0.314 mA. Then, the cells were potentiostatically charged at 2.35 V until the current was below $1\times10^{-5}$ A.

## DFT calculation

Density Functional Theory (DFT) calculations using the dmol3 package, we first optimize the material structure, then calculate the electron density, electrostatics, density of states, and adsorption energy information. Using the Perdew-Burke-Ernzerhof (PBE) exchange-correlation functional within the generalized gradient approximation (GGA) to describe the exchange-correlation energy. The convergence criteria for total energy and force on each atom were set as $10^{-5}$ eV and 0.07 Ha $Å^{-1}$, respectively. And k-points grid parameters are 1×1×1. The adsorption energy was calculated with the equation: $E_{ads} = E_{A+B} - (E_A + E_B)$, where $E_{ads}$ is the adsorption energy, $E_A$, $E_B$, $E_{A+B}$ are the total energy of the geometry-optimized substrate, adsorbate, and the adsorption system models, respectively.

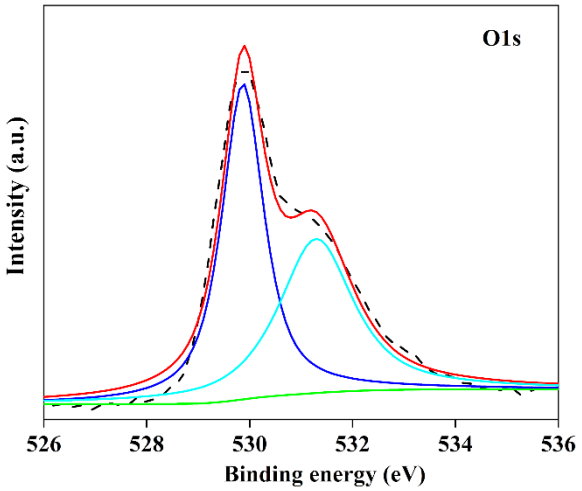


Fig. S1 O1s spectrum of Zn-CSN@$MnO_2$ powder.

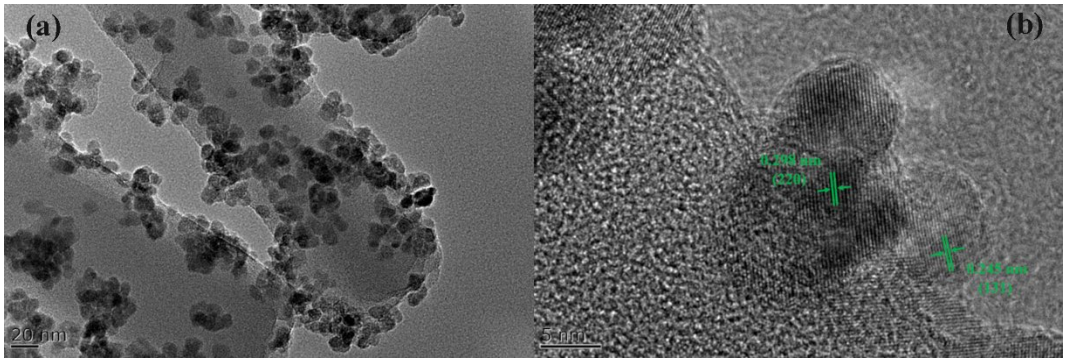


Fig. S2 High-resolution TEM and local magnification of Zn-CSN@$MnO_2$ (the (220) crystal plane of Zn-CSN and the (131) crystal plane of $MnO_2$ were shown in Figure b).

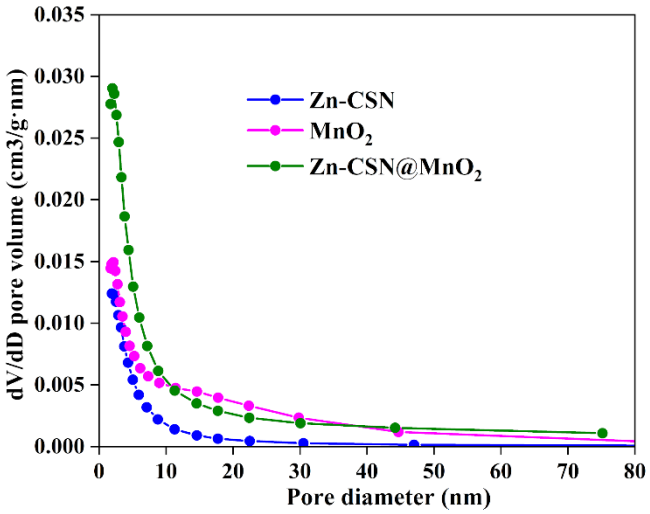


Fig. S3 Pore distribution of Zn-CSN@$MnO_2$, Zn-CSN, and $MnO_2$.

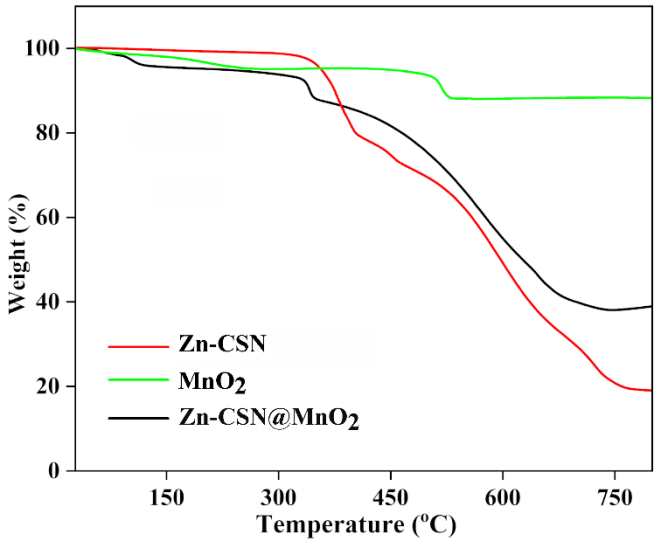


Fig. S4 TGA curves of Zn-CSN@$MnO_2$, Zn-CSN, and $MnO_2$.

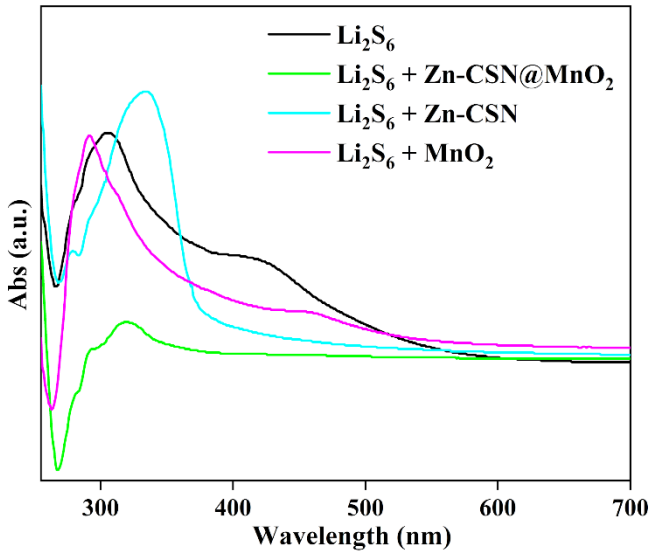


Fig. S5 Ultraviolet spectrum of adsorbed $Li_2S_6$ solution.

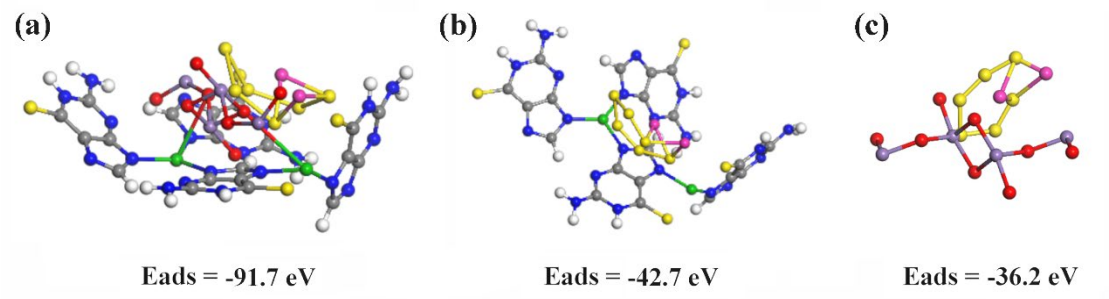


Fig. S6 $Li_2S_6$ adsorption energy of (a) Zn-CSN@$MnO_2$; (b) Zn-CSN; (c) $MnO_2$.

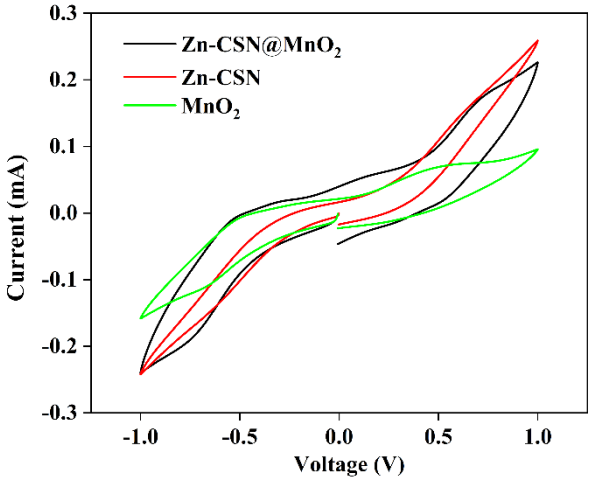


Fig. S7 Cyclic voltammetry curves of symmetrical cell.

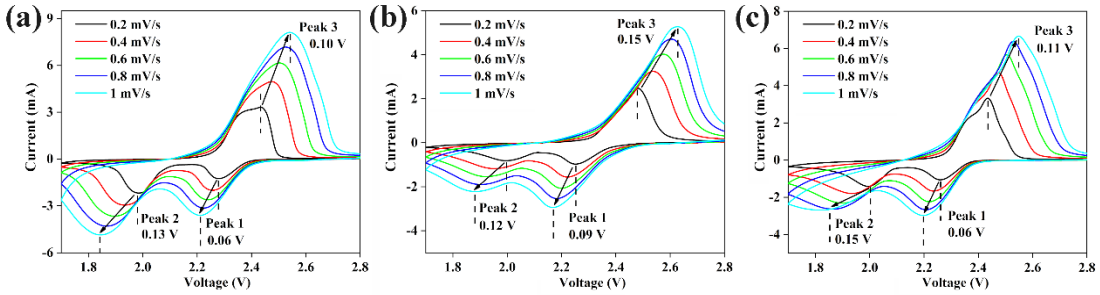


Fig. S8 Cyclic voltammetry curves at different scan rates: (a) Zn-CSN@$MnO_2$; (b) Zn-CSN; (c) $MnO_2$.

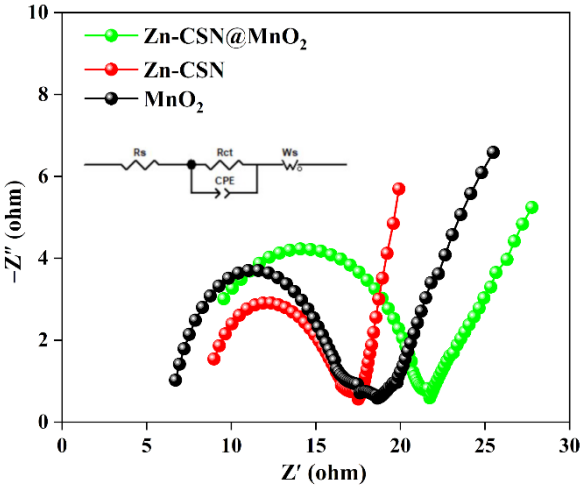


Fig. S9 Electrochemical impedance spectroscopy after 30 cycles at 0.2C.

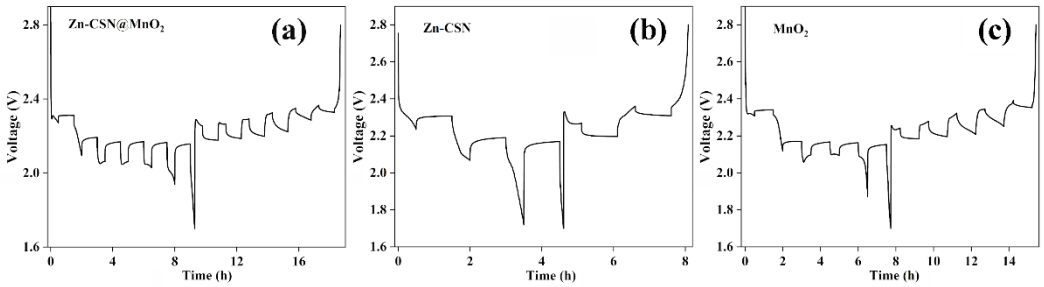


Fig. S10 GITT curves of Zn-CSN@$MnO_2$, Zn-CSN, and $MnO_2$.

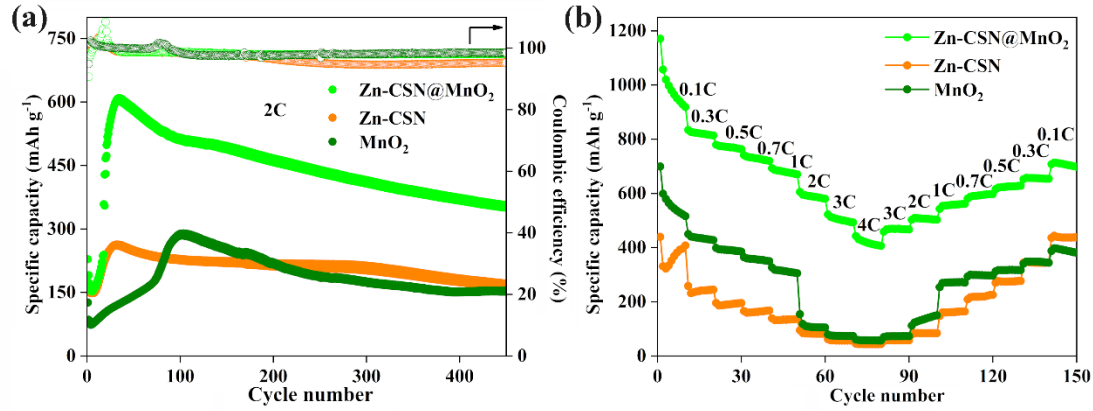


Fig. S11 Electrochemical performance of Zn-CSN@$MnO_2$, Zn-CSN, $MnO_2$: (a) cycling performance at 2C; (b) rate performance.

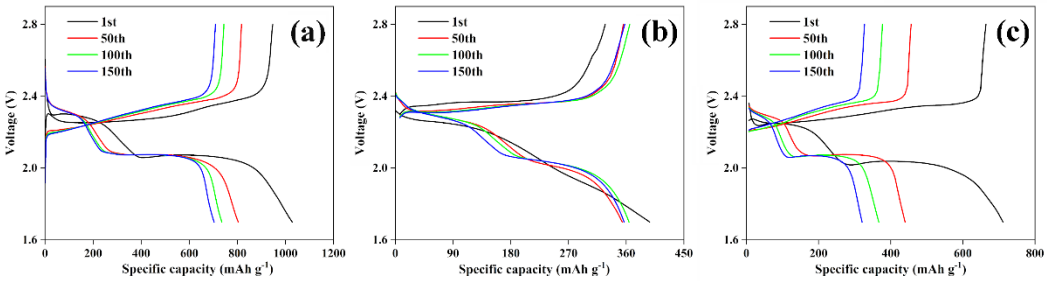


Fig. S12 Galvanostatic discharge/charge curves of (a) Zn-CSN@$MnO_2$; (b) Zn-CSN; (c) $MnO_2$ at 0.5C.

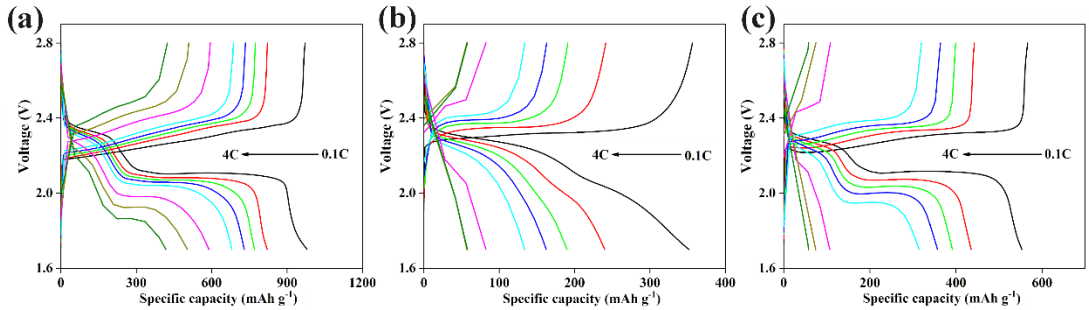


Fig. S13 Discharge and charge curves at different rates: (a) Zn-CSN@$MnO_2$; (b) Zn-CSN; (c) $MnO_2$.

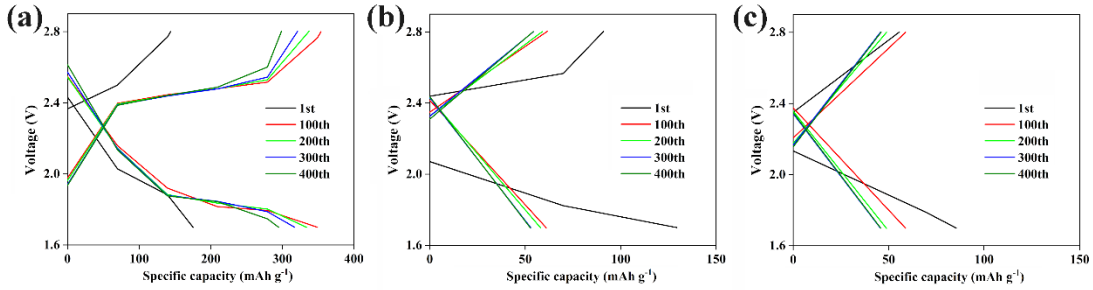


Fig. S14 Discharge and charge curves at 5C: (a) Zn-CSN@$MnO_2$; (b) Zn-CSN; (c) $MnO_2$.

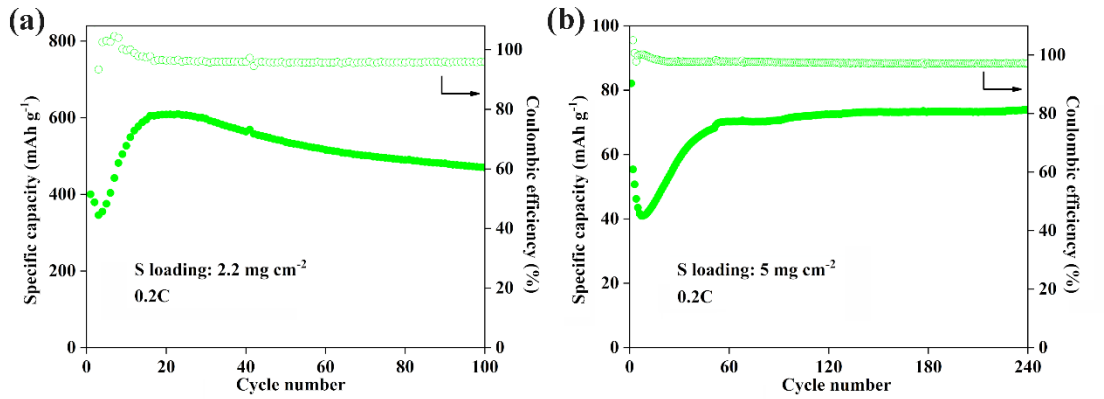


Fig. S15 Electrochemical performance of Zn-CSN@$MnO_2$ at high sulfur loading. (a) S solading-2.2 mg $cm^{-2}$; (b) S loading-5 mg $cm^{-2}$.

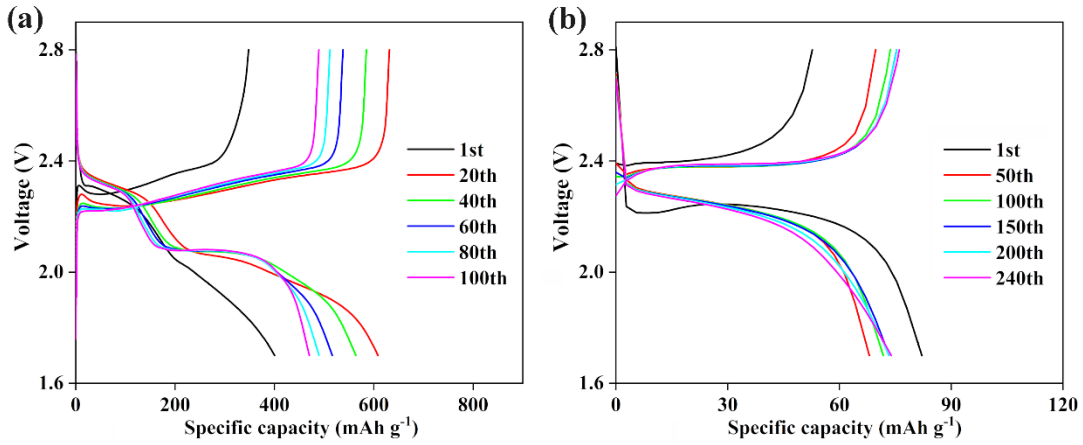


Fig. S16 Galvanostatic discharge/charge curves of Zn-CSN@$MnO_2$ at 0.2C for high sulfur loading. (a) S solading-2.2 mg $cm^{-2}$; (b) S loading-5 mg $cm^{-2}$.

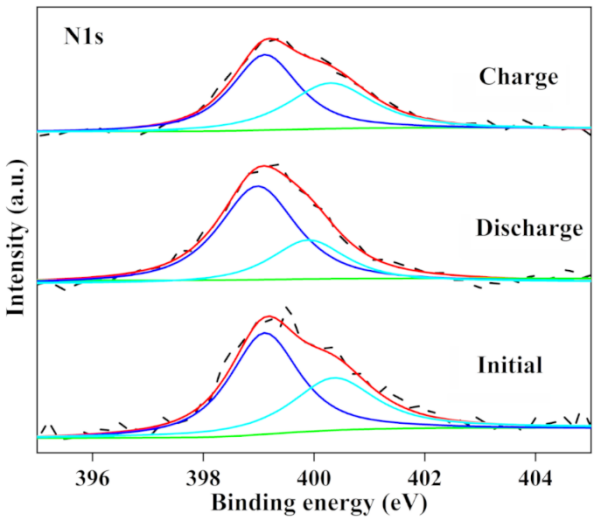


Fig. S17 *Ex-situ* XPS spectra of Zn-CSN@$MnO_2$ electrode before and after first cycle: N1s.

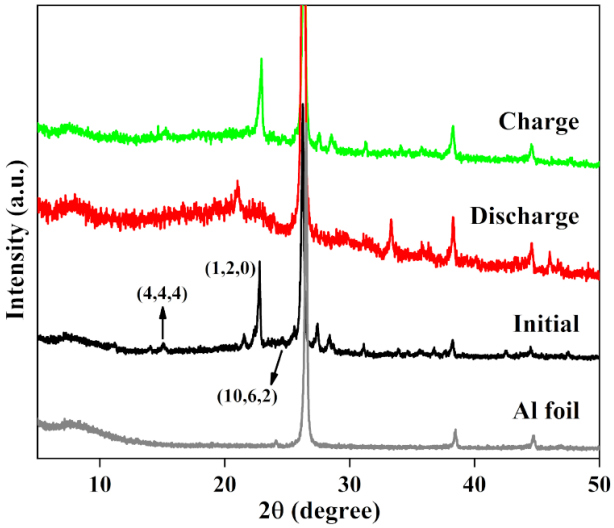


Fig. S18 *Ex-situ* XRD of Zn-CSN@$MnO_2$ electrode before and after first cycle.

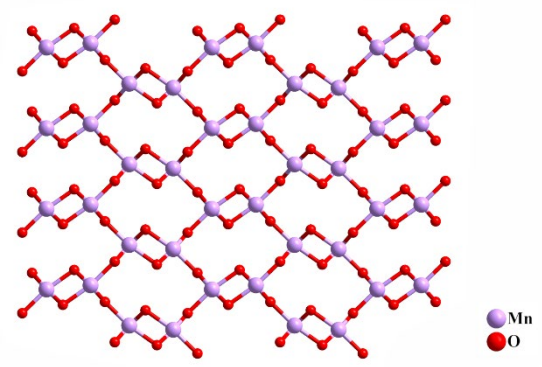


Fig. S19 The structure of γ-$MnO_2$.

Table S1. Lithium-ion diffusion coefficient ($D_{Li+}$) of materials.

| Composites | $D_{Li+}$ of discharge stage ($cm^2\ s^{-1}$) | $D_{Li+}$ of charge stage ($cm^2\ s^{-1}$) |
|---|---|---|
| Zn-CSN@$MnO_2$ | $1.5 \times 10^{-17} \sim 1.5 \times 10^{-13}$ | $4.9 \times 10^{-15} \sim 1.3 \times 10^{-13}$ |
| Zn-CSN | $2.7 \times 10^{-22} \sim 3.3 \times 10^{-20}$ | $6.5 \times 10^{-20}$ |
| $MnO_2$ | $7.8 \times 10^{-21} \sim 4.9 \times 10^{-18}$ | $8.3 \times 10^{-20} \sim 4.3 \times 10^{-18}$ |

Table S2. Electrochemical performance comparison of manganese dioxide and MOFs materials in lithium-sulfur batteries.

| Composites | Current density (C) | Capacity (mAh $g^{-1}$) | Reference |
|---|---|---|---|
| $MnO_2$@HCS | 1 | 705 | [1] |
| $MnO_2$ NW/EG | 1 | 538 | [2] |
| $MnO_2$/NPC | 1 | 624.4 | [3] |
| $MnO_2$@HA | 1 | 665 | [4] |
| $MnO_2$-HC | 0.2 | 663 | [5] |
| CoNi-MOF | 0.2 | 690 | [6] |
| Ni-HHTP@CP | 0.2 | 910 | [7] |
| Cu-BTC/CNTs | 1 | 485.9 | [8] |
| DLHC/S@$MnO_2$-ACNT | 1 | 430 | [9] |
| $MnO_2$@PE | 1 | 665 | [10] |
| AC $MnO_2$ | 1 | 513.24 | [11] |
| **Zn-CSN@$MnO_2$** | **5** | **294.97** | **This work** |

# References


1 Q. Shao, D. Guo, C. Wang and J. Chen, *Journal of Alloys and Compounds*, 2020, **842**, 155790.

2 Q. Li, Z. Ma, J. Zhao, K. Shen, T. Shi, Y. Xie, Y. Fan, X. Qin and G. Shao, *Journal of Power Sources*, 2022, **521**, 230929.

3 M. Hou, K. Chen, G. Zhang, X. Liang, X. Liu and S. Xing, *Journal of Energy Storage*, 2023, **72**, 108339.

4 X. Ding, R. Gu, P. Shi, Q. Xu and Y. Min, *Journal of Alloys and Compounds*, 2020, **835**, 155206.

5 Y. Zhang, L. Ma, R. Tang, F. Zhao, S. Niu, W. Su, C. Pan and L. Wei, *Applied Surface Science*, 2022, **585**, 152498.

6 X. Ren, Q. Wang, Y. Pu, Q. Sun, W. Sun and L. Lu, *Advanced Materials*, 2023, **35**, 2304120.

7 S. Wang, F. Huang, Z. Zhang, W. Cai, Y. Jie, S. Wang, P. Yan, S. Jiao and R. Cao, *Journal of Energy Chemistry*, 2021, **63**, 336-343.

8 T. Deng, X.-L. Men, X.-C. Jiao and J. Wang, *Ceramics International*, 2022, **48**, 4352-4360.

9 Y. Ren, J. Hu, H. Zhong and L. Zhang, *Colloids and Surfaces A: Physicochemical and Engineering Aspects*, 2023, **667**, 131408.

10 Y.-W. Tian, Y.-J. Zhang, L. Wu, W.-D. Dong, R. Huang, P.-Y. Dong, M. Yan, J. Liu, H. S. H. Mohamed, L. H. Chen, Y. Li and B.-L. Su, *ACS Applied Materials & Interfaces*, 2023, **15**, 6877-6887.

11 Y.-T. Gao, X.-Y. Wang, D.-Q. Cai, S.-Y. Zhou and S.-X. Zhao, *ACS Applied Materials & Interfaces*, 2023, **15**, 30152-30160.